Int. J. Electrochem. Sci., 16 **(2021)** Article ID: 21047, doi: 10.20964/2021.04.25

International Journal of
ELECTROCHEMICAL
SCIENCE
www.electrochemsci.org

Erosion-Corrosion Resistance and Electrochemical Behavior of AZ31 Magnesium Alloy Processed by Equal Channel Angular Pressing (ECAP)

Osama M. Irfan[1,2]

[1] Departments of Mechanical Engineering, Qassim University, Saudi Arabia
[2] Department of Mechanical Engineering, Beni Suef University, Egypt
E-mail: osamaerfan@qec.edu.sa

Received: 2 December 2020 / *Accepted:* 19 January 2021 / *Published:* 28 February 2021

The current work studies the effect of Equal Channel Angular Pressing (ECAP) on the erosion – corrosion (E-C) resistance and electrochemical behavior of Magnesium AZ31 Alloy. Samples of AZ31 alloy were subjected to ECAP process up to four passes at 200 ^{o}C. The Vickers micro hardness, Hv had been measured and the structural homogeneity was assessed. Microstructural images by optical microscopy were evaluated. The E-C tests by slurry pot method through weight loss and electrochemical analysis had been conducted. Simulated sea water with silica sand particles was used in the E-C experiments. Scanning electron microscope SEM was employed to investigate the samples after E-C. The potentiodynamic polarization was achieved from a simulated sea water solution (3.5% NaCl) and electrochemical impedance spectroscopy was carried out on the solution to examine the surface properties of the samples. The effects of flow velocity and testing time on the weight loss due to E-C at different ECAP passes were investigated. The results indicated an increase in hardness after four ECAP passes with substantial structural homogeneity. For all velocities, the weight loss of samples subjected to ECAP is lower compared to the original samples. It is obvious that the time has a serious effect on the E-C resistance of AZ31 alloy. For samples subjected to ECAP, time has less influence on material removal.

Keywords: AZ31 magnesium alloy; ECAP; Erosion-corrosion; Electrochemical

1. INTRODUCTION

Magnesium alloys are mainly used for transportation industries due to the reduction in weight that can be accomplished. AZ31 magnesium alloys address a lot of potentials and challenges for effective use in automotive, non-automotive, and biomedical applications [1]. The erosion – corrosion (E-C) resistance and mechanical properties of AZ31 alloy, as a metallic alloy, are affected by the processing of the material [2]. Severe plastic deformation (SPD) in processing metals is a successful technique to achieve substantial grain refining with microstructures of grain sizes within either micrometer or

nanometer scale [3]. Equal-channel angular pressing (ECAP) is one of the most common and attractive methods of SPD because it is easy to conduct and effective for producing large samples or products [4] . Moreover, E-C resistance is one of the major issues in engineering studies because it considerably affects the performance and service life of the structural components. Therefore, considerable attention has been devoted to the examination of the E-C behavior of different materials in order to mitigate the deterioration of surface components by choosing proper materials [5, 6]. Normally, when ECAP is applied on a certain material the results concentrate on the microstructural advancement and the mechanical properties as well as thermal stability of the developed materials. This is a significant weakness, as E-C behavior is of great concern in several applications [7]. The homogeneity of the material can be assessed by measuring the micro hardness and surface properties can be examined through the investigation of E-C behavior [8]. This approach can be used with a variety of materials such as copper, copper alloys, pure aluminum, and aluminum alloys [9, 10, 11]. Many studies have reported improved wear resistance by using ECAP [12]. As an example, experiments on titanium have shown that ultrafine grained samples revealed better wear resistance over coarse grained titanium [13]. However, in some cases, the wear resistance of the ultrafine grained materials obtained by ECAP was stated to be lower than that of the coarse grained materials [14]. Important research attempts have been made to understand the influence of multiple parameters on the E-C response of various metallic materials [15, 16] . In order to clarify the behavior of the E-C interaction two mechanisms were reported [17, 18]. The first includes corrosion-enhanced erosion and is related to the destruction of surface hardness or material strength. The second explains the erosion-enhanced corrosion which is triggered by a delay in the coating film on the metal surface [19]. In addition, electrochemical methods have been commonly used to examine the resistance of materials to corrosion. These methods, such as the electrochemical impedance spectroscopy (EIS) process, have been shown to be an effective tool for understanding the corrosion behavior of metallic materials [20]. The studies on E–C of 1018 carbon steel showed that the presence of high salt concentration (NaCl) above a certain critical level (3.5 % wt.) resulted in a reduced erosion rate. Other Numerous studies have shown that the maximum E–C rate for some materials, such as 304 stainless steel and aluminum, arises at impingement angle ranging from 25° to 45° [21, 22]. The corrosion behavior of Cu-10Sn bronzes in aerated chloride media has also been studied [23, 24]. The E-C of aluminum-brass alloys at several attack angles was also investigated and the results revealed that the erosion enhanced corrosion rate exhibited values more than 50% of the entire erosion-corrosion rate [25]. It is well known that E-C is a complex phenomenon, which comprises the interaction between a mechanical processes (erosion) and an electrochemical processes (corrosion). The factors for the E-C behavior of materials are the velocity of the flow, impact (attack) angle, erodent particle mass, and solid particle concentration [26, 27]. To date, no relevant measurements were reported for magnesium AZ31 alloy although this knowledge is required within the range of so-called hard-to-work materials [28, 29].The findings indicated that AZ31 alloy with a grain size of 9.4μm produced a bimodal distribution of grain in ECAP with a gradual evolution towards a homogeneous grain structure with more straining [30].

To date, no adequate results are available to verify the effect of ECAP on the E-C behavior of AZ31 alloy. The present work emphasizes on correlating the E-C behavior and microstructural changes of the AZ31 alloy after the application of ECAP. This alloy was selected based on several reports of the

AZ31 alloy subjected to ECAP [31, 32] and it is rational to asses or expect results that the grain refinement affects the mechanical and surface properties of the materials.

2. EXPEREMENTAL WORK

2.1 Materials and Methods

The experimentations were implemented on a AZ31 magnesium alloy having a chemical composition (wt. %) shown in Table 1.

Table 1. Chemical Composition of AZ31 Magnesium Alloy

Element	Al	Zn	Mn	Si	Mg
% wt.	3.1	0.75	0.25	0.02	Bal

The cylindrical samples were subjected to the extrusion process in a temperature range of 350 – 450 ^{o}C into diameters of 20 mm. The produced samples of 150 mm lengths were subsequently prepared for ECAP. Initially, microstructural inspection showed an average grain size of ~20 – 30µm [33]. In order to avoid the grain growth during ECAP no annealing was conducted before the processing [34].

2.2 ECAP Process & Microhardness Measurements

The ECAP was applied using a split die having a 90o channel with a diameter of 20 mm. More details of the die specifications and the process were presented in previous works [35, 36]. The ECAP process was conducted to a maximum of 4 passes at a temperature of $200^{\pm 20}$ ^{o}C with a strain rate of 0.5 mm/min using a route BC in which the samples are rotated by 90◦ about their axes after each pass [37]. A hydraulic press of 160 tons capacity was used for pressing. Figure1 illustrates the principle of ECAP process.

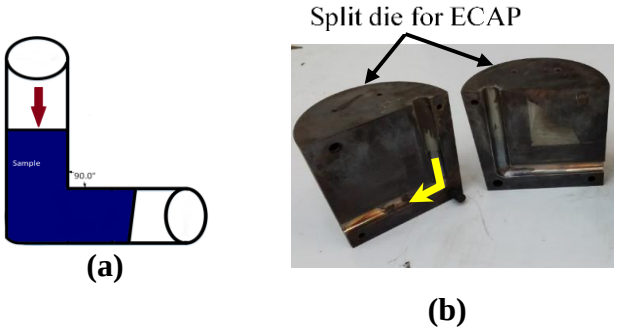

Figure 1. (a) ECAP Principle, (b) Die used in ECAP

To evaluate the variations in Hv values along the cross section of samples, the hardness was measured following two techniques. First, measurements had been considered at locations along the line

intersecting the cross-sections perpendicular to the top of each sample to monitor the variations in hardness after pressing. These records were considered at points of 0.5mm apart. The average of Hv at each location obtained by averaging three measurements around the selected location. Second, records were taken over the surface following a straightforward pattern in which each location was separated from the neighboring points by a distance of 0.5 mm either vertically and horizontally. The values of the micro hardness were reported on a sample in the original condition before ECAP.

2.3 Electrochemical & Erosion-Corrosion Experiments

In order to conduct the electrochemical and erosion- corrosion (E-C) experiments the surface of each AZ31 sample was polished by 600 grits SiC emery papers, cleaned in alcohol and distilled water, and dried by a stream of cold air. E-C tests were carried out through a slurry pot setup described in Figure 2. The erosive liquid was a solution of simulated sea water of 3.5 % NaCl containing SiO_2 particles (concentration of 20%wt.) of an average size of 300 - 400 μm. The flow velocity of 5, 7, 9 and 12 m/s was applied by controlling the revolution speed of the rotating shaft (impeller) [38]. The overall test period was 12hours and the weight loss was recorded every 2hours using a digital microbalance of 0.1 mg accuracy. The electrochemical experiments were conducted at 50°C, a cylindrical shape platinum was used as an auxiliary electrode, and Ag/AgCl was used as a reference electrode during experiments.

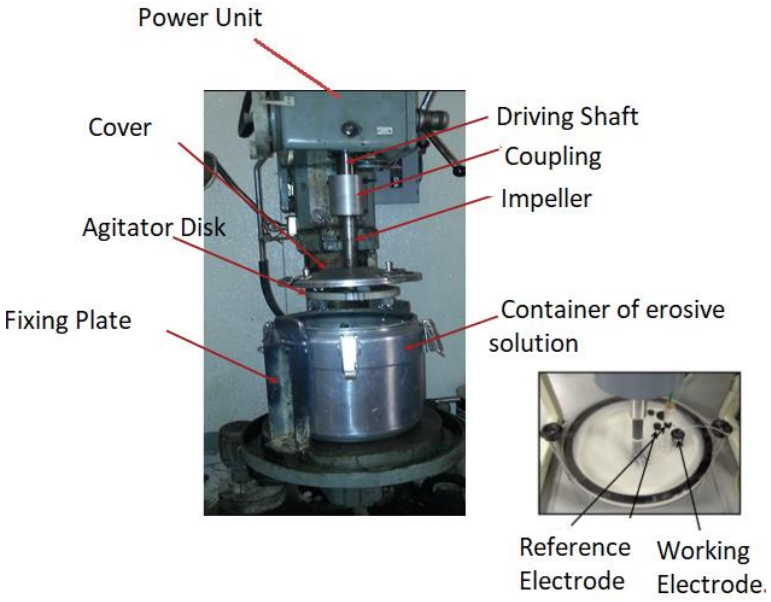

Figure 2. Setup of the Erosion-Corrosion and Electrochemical Corrosion Experiments [39]

Measurements of electrochemical impedance spectroscopy and potentiodynamic polarization were performed at different intervals. Electrochemical impedance spectroscopy were performed at the open-circuit potential with a disturbance amplitude of 10 mV rms and a range of frequency of 200 kHz to 4 MHz The potentiodynamic polarization curves were developed from 40 mV of cathode over potential to 500 mV of anodic over potential relative to the open-circuit potential using a scan rate of

0.165 mV/s. Electrochemical impedance spectroscopy and potentiodynamic polarization were carried out using CS350 electrochemical workstation. In order to investigate the morphology variation of AZ31 alloy, the surfaces were assessed by scanning electron microscopy (SEM) with a JEOL JSM 2490 apparatus.

3. RESULTS and DISCUSSION

3.1. Microhardness Results

The microhardness values were recorded and plotted along the distance from the bottom of the sample processed by ECAP as shown in Figure3. The lower dotted line illustrates the trend of microhardness of the extruded samples before ECAP. The error bars are not presented because the error values are small and the bars might be unnoticed. However, the calculations presented the average error at 95% confidence level were ~1.4, ~2.1, ~1.8, and ~1.2Hv after pressing through 1, 2, 3, and 4 passes, respectively.

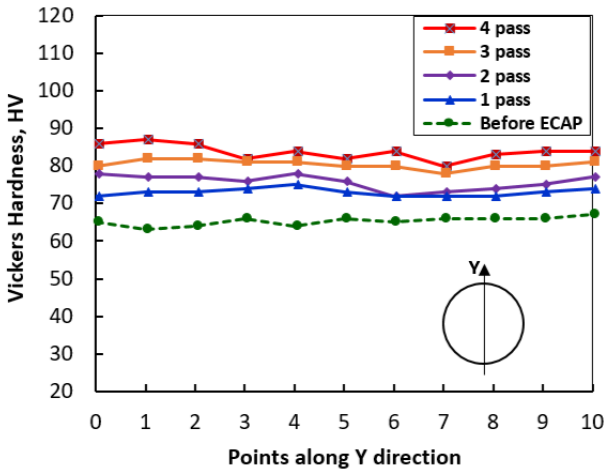

Figure 3. Vickers microhardness (HV) of AZ31 samples processed by ECAP

The measurements in Figure 3 shows that microhardness is increasing significantly after the first ECAP pass, continues to rise to 2 passes and then stays relatively steady when the sample is subjected to 4 passes. It is also obvious that the microhardness values vary along the Z direction (longitudinal direction of samples) with a deviation from the mean of almost ±4Hv after 2 passes but approximately ±3Hv after 4 passes. These deviations are substantial as they are larger than the estimated mean error of ±2. Hence, the findings showed an improvement of the microstructural homogeneity with increasing numbers of ECAP passes. After one ECAP pass a higher microhardness across the whole section is experienced. After four ECAP passes, the sample has attained a rational homogeneity in the distribution of microhardness with a mean of 85 HV but with some specific areas with higher hardness values of 90Hv. Finally, there is an enhancement in homogeneity after 4 passes. This can be attributed to the high strains generated due to ECAP. A variety of grain boundaries is available in such a way that arrays of

enlarged cells are developed within each grain after one pass of ECAP and these new cells grow into arrays of ultrafine grains isolated by boundaries with high angles of dislocation [40]. As a result, the grain refinement of AZ31 alloys is triggered at the preceding boundary so that, if the original grain size is fairly substantial, this contributes to the creation of a homogeneous grain structure after ECAP passes. Thus the centers of higher initial grains are not instantaneously absorbed by the initiation of smaller grains [41]. The current findings are consistent with this system and verify the potential to deliver good homogeneity after an appropriate number of ECAP passes. The results also are compatible with the approach that homogeneous grain distributions are transitional in nature and become homogeneous when the material is subject to a considerable number of ECAPs [42].

3.2. Microstructural Observations

The microstructure was inspected by an optical microscopy and the samples were prepared by the standard technique through the sanding with SiC emery papers, polished with alumina suspension solution, and then etched in a solution of 4 vol. % concentrated HNO_3. The original AZ31 alloys had a rough grain structure. However, microscopic homogeneous, and fine-grained structures created at higher deformation. The grain size was determined by means of both linear intercept method and Image software [43]. Grain refining took place due to the deformation generated by ECAP. The microstructures of AZ31 alloy are shown in Figure 4a-d where (a), corresponds to the initial samples before ECAP.

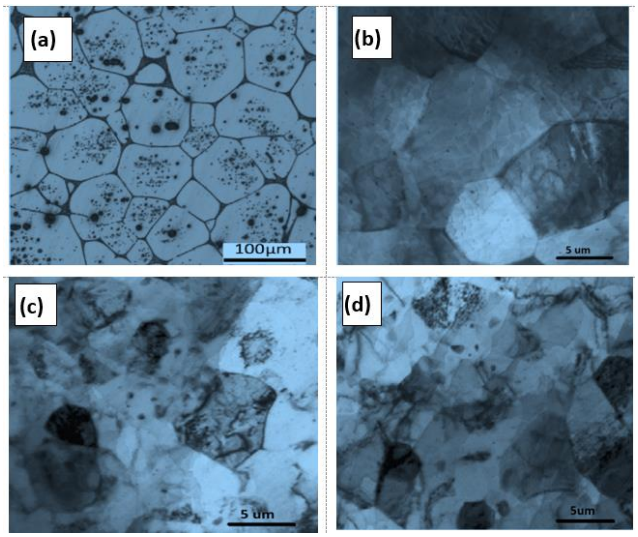

Figure 4. Microstructure variation of AZ31 alloy along ECAP passes (a) Extruded sample before ECAP, (b) 1 pass, (c) 2 pass, (d) 4 pass

It can be noted that larger grain sizes obtained even by lower magnification. The average grain size was calculated by determining at least 15 different grains and then approximating the 95% confidence limits. Since the original grain size for the alloy was ~25–35µm prior to ECAP, these dimensions show that the grain size is reduced considerably after the first ECAP pass as shown in Figure4 (b). It follows from examination of Figure 4(c) that the grains were clearly obtained as curvy

and poorly outlined. Similar findings were achieved for other alloys subjected to ECAP such as aluminum alloys and they were understood as revealing of the existence of non-equilibrium grain boundaries [44]. It is realistic to expect that the relatively large original grain size of ~25–35µm is enormous to attain a homogeneous microstructure after only one ECAP pass. Figure 4(d) represent the microstructure of samples pressed through 4 passes. A similar grain size of Figure4(c) was noted, thereby approving the homogeneity attained in the AZ31 alloy after 4 ECAP passes [45].

3.3 Electrochemical and Erosion-Corrosion Findings

3.3.1 Electrochemical analysis

The dynamic polarization curves of the AZ31 alloy for various ECAP passes in simulated sea water with 20% wt. of silica particles are shown in Figure 5.

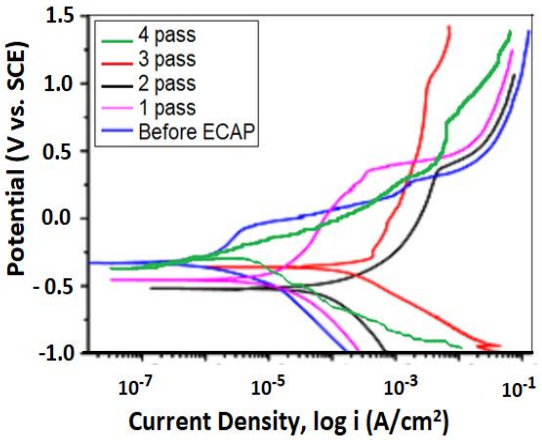

Figure 5. Potentiodynamic polarization curve of AZ31 alloy in simulated sea water solution

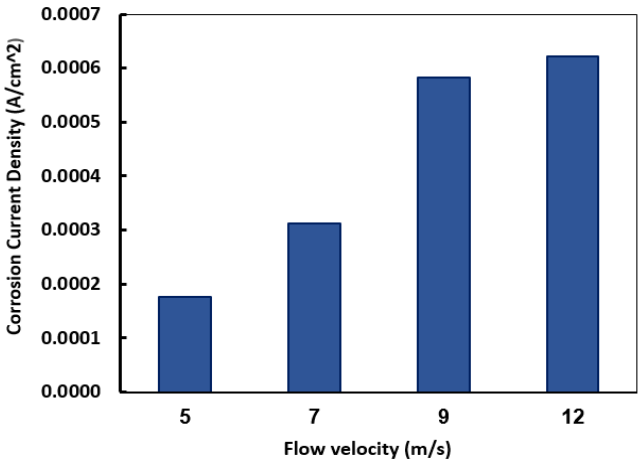

Figure 6. Corrosion current density of AZ31 alloy as a function of the flow velocity.

The corrosion potential was between −0.10V and 1.25V, and the results revealed the same trend for all passes. Figure 5 and Figure6 illustrate that the corrosion resistance enhances with the increasing of ECAP passes, compared to the original sample. However, no specific configuration was perceived in the case of corrosion potential (Figure5). The extruded original samples exhibited highest potential values compared to the samples subjected to ECAP, which can be clarified in Figure 4a-d and Figure 10. The corrosion current densities were obtained through linear extrapolation, as presented Figure 6. It can be observed that the corrosion rate of the AZ31 alloy increased steadily as the flow velocity increased.

More grain refinement of AZ31 alloy was achieved after each ECAP pass and more sites are candidate to initiate corrosion and thus rises the corrosion rate, which declines the overall corrosion resistance. The grain refining does provide more corrosion areas either within the grain boundary or surrounding to the grain boundaries [46]. Figure 7 and Figure 8 comprise the Bode value and the Bode phase plot, respectively, in simulated sea water. The Bode magnitude plot has two zones as shown in Figure 7. The plot shows constant log |Z| values vs. log frequency in the lower-and higher-frequency zones, indicating the response to the solution resistance. In the wide (0.1−1000.0 Hz) mid-frequency range, the spectra showed a slightly linear slope. This is the characteristic reaction of the capacitive behavior of the surface. The phase angle of the original extruded AZ31 alloy samples (Figure8) were approached by 65^{o} - 70° in the Bode phase plot at the middle frequency range. For the other samples (first, second, third, and fourth ECAP passes), the phase angle fallen considerably to almost 45°, showing a surface diffusion that affected the resistance of the solution and therefore dropped the resistance to corrosion.

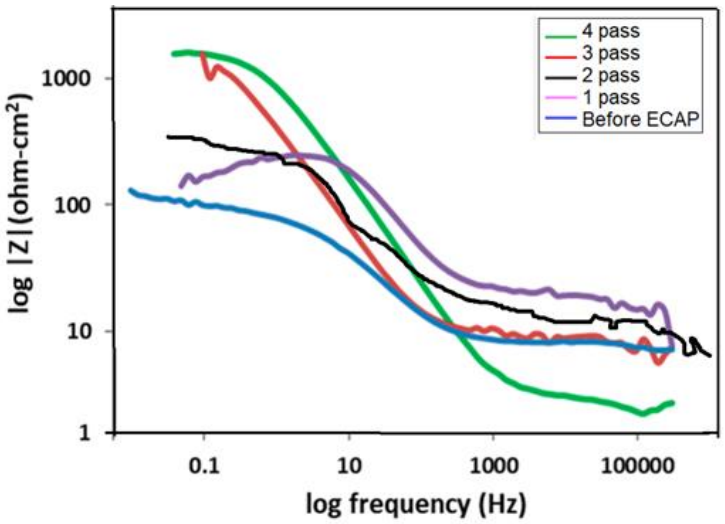

Figure 7. Electrochemical impedance spectroscope curve of AZ31 alloy processed by ECAP passes

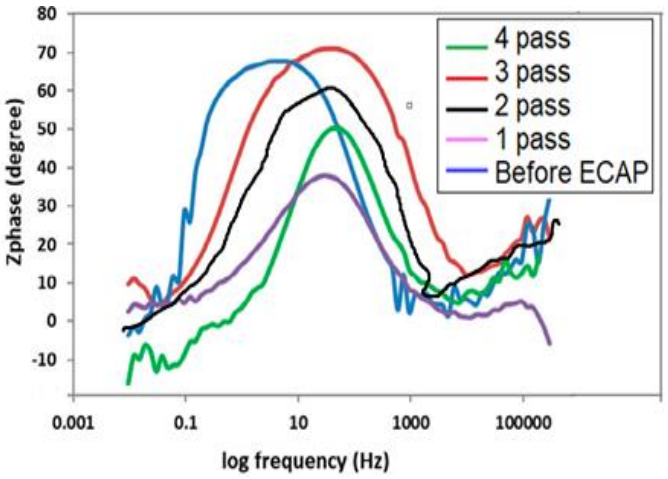

Figure 8. Electrochemical impedance spectroscope Bode angle plot of the AZ31 alloy in simulated sea water

Figure 9 illustrates an equivalent electric circuit from which the parameters of the process can be achieved. The main parameters are RS, RL, L, RCT, and CPE, which designate the solution resistance, electrical inductance, inductance element, charge transfer resistance, and constant phase element, respectively. The early stage of corrosion can be specified by RL and L [47]. The polarization resistance (RP) of AZ31 alloy is inversely proportional to the corrosion opposition. It was noticed that the corrosion resistance of the original samples (before ECAP) was greater than that of the ECAP samples.

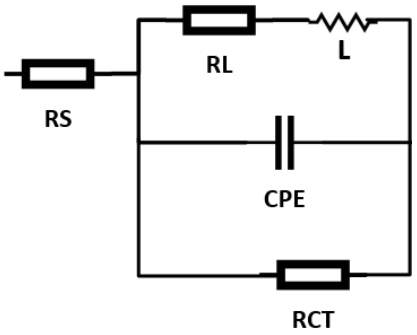

Figure 9. Equivalent electrical circuit for electrochemical impedance spectroscope parameters

Table 2 displays the values of the parameters (RS, RL, L, RCT, and CPE). It is clear that, the ECAP has a little influence on the surface properties during the corrosion. It was found that after ECAP the polarization resistance was less than that in the original samples. Under different ECAP passes, a greater values of RP were achieved in the original sample compared to the ECAP ones [48].

Table 2. Parameters of Electrochemical Impedance Spectroscopy in Sea Water Solution

ECAP Condition	Solution Resistance RS ($\Omega.cm^2$)	Electrical Inductance RL ($\Omega.cm^2$)	Inductance Element L (H/cm^2)	Charge Transfer Resistance RCT ($\Omega.cm^2$)	Constant Phase Element CPE ($\mu F \cdot S^{(n-1)}$)/ cm^2
No ECAP	25.10	2214	1978	2436	30.41
1 Pass	21.83	512	411	2262	35.23
2 Pass	24.32	386	266	2138	52.63
3 Pass	23.69	223	195	1689	56.42
4 Pass	22.98	176	112	1454	48.18

3.3.2 SEM observations

SEM assessment were conducted for AZ31 alloy samples before and after ECAP. For the samples before ECAP process (Figure 10(a)) the micro cracks and relatively big semicircular pits appeared on the surface as a result of the flow velocity and corrosion that destroying the surface. Moreover, E-C resistance is lower than the rate of removal of material during the flow movement. For samples subjected to 4 ECAP passes, rectangular small pits were observed in the grain boundaries as an evidence of galvanic cells. The amount of galvanic cells increased with increasing ECAP passes as displayed in Figure 10(b). Thus, electrochemical corrosion plays a very important role in removing the material by targeting the relatively weak surface layer. The oxide layer generated on the surface are relatively stable in AZ31 due to aluminum contents in the alloy [49, 50].

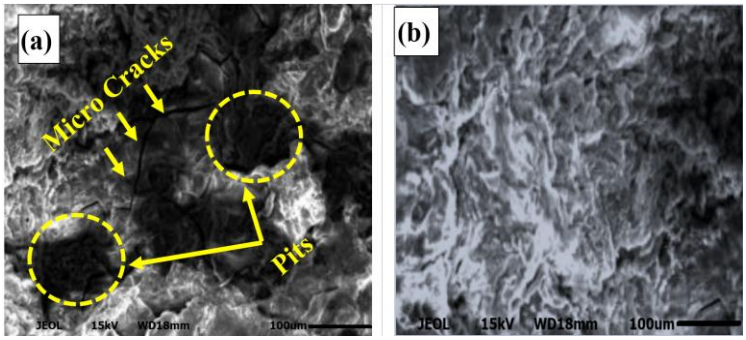

Figure 10. SEM images of AZ31 alloy surface after Erosion-Corrosion (a) before ECAP (b) After ECAP (4 pass)

3.3.3 Erosion-corrosion results

The effect of flow velocity on the E-C at various ECAP passes is displayed in Figure 11. It can be noticed that the maximum weight losses for original AZ31 samples before ECAP and samples subjected to ECAP (4 passes) were 9 $x10^{-6}$ and $4x10^{-6}$ g/mm^2, respectively (55.5 % improvement in E–C resistance was achieved). The weight loss rises with increasing the flow velocity for all cases. More material removal from the AZ31 surface was experienced as a result of sand particles suspended in the

slurry (erosion effect). The erosive solid particles act as a medium that causes kinetic energy influencing the surface. However, for all velocities, the weight loss of samples subjected to ECAP is lower compared to the original sample.

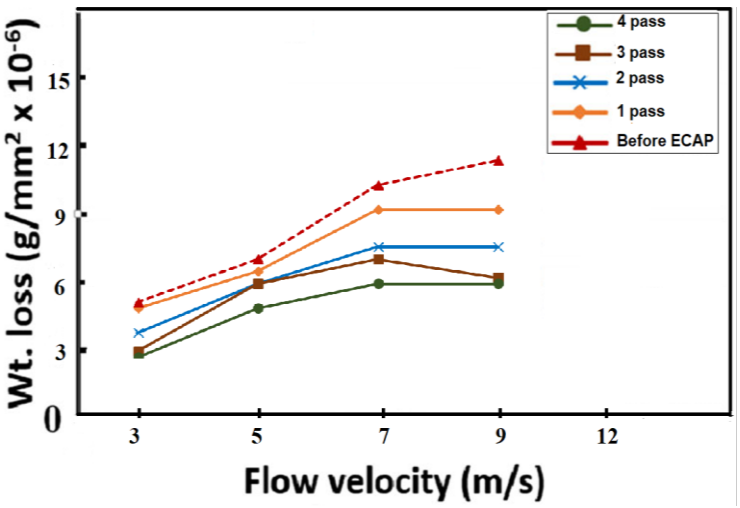

Figure 11. E-C of AZ31 alloy subjected to ECAP as a function of flow velocity (Time = 12 hr)

Figure 12 presents the effect of duration on the E-C of AZ31 alloy, both before and after ECAP. The experiments were done for several durations at a constant linear velocity of 9 m/s and an exposure angle of 45º.

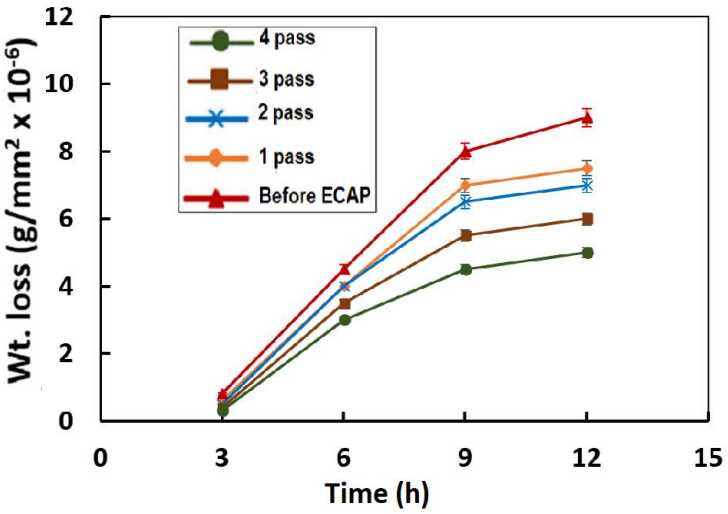

Figure 12. E-C of AZ31 alloy subjected to ECAP as a function of time (Flow velocity = 9 m/s)

It is obvious that the time has a serious effect on the E-C resistance of AZ31 alloy. For original samples, before ECAP, the weight loss was $8x10^{-7}$, $4.3x10^{-6}$, $8x10^{-6}$, and $9.2x10^{-6}$ g/mm^2 at 3, 6, 9, and 12 hours, respectively. Significant increase is observed from 3 to 9 hours but small difference was

observed from 9 to 12 hours. For samples subjected to ECAP, time has less influence on material removal. After 4 ECAP passes, the weight losses were $3x10^{-7}$, $3.3x10^{-6}$, $4.2x10^{-6}$, and $5x10^{-6}$ g/mm^2 at 3, 6, 9, and 12 hours, respectively. The improvement in E-C resistance can be understood as follows. During the ECAP process, the micro hardness (Hv) rises gradually. Thus, the weight loss of the samples that subjected to ECAP decreased. Similar trends were obtained earlier when the influence of time on E–C of copper, aluminum, and Al-Si alloy were examined [51].

4. CONCLUSIONS

In this research, samples of magnesium AZ31 alloy had been subjected to ECAP at 200 ºC for up to 4 passes. Vickers micro hardness, Hv, was measured on cross-section of the circular samples after ECAP and microstructural investigation by optical microscopy and SEM were performed. The obtained results depicted a reduction in grain size, an increase in the microhardness, and inhomogeneity after the first ECAP pass. However, a trend towards a further homogeneous structure and less grain size after 4 ECAP passes was observed. Moreover, the corrosion resistance of the samples after ECAP exhibited a different trend compared to the original samples (before ECAP), due to the grain refinement along the first to fourth ECAP passes. The corrosion rate in terms of weight loss of the samples after ECAP increased as a result of grain refinement, which formed more positions for originating corrosion and then reduced the corrosion resistance. Increasing the ECAP passes causes serious degradations of AZ31 surface due to the reduction in the resistance to corrosion. However, an improvement of E-C resistance was perceived after four ECAP passes. In addition, increasing the flow velocity of the slurry and testing time leads to increasing the kinetic energy of the particles when striking the samples, thus accelerating the weight loss of both samples before and after ECAP.

ACKNOWLEDGEMENTS
The author is grateful to Eng. Yasser Alshutaif and Mr. Abdurrahman Elgherir for their effort in carrying out the ECAP process and for preparation of the samples. Also thanks are extended to Qassim University, Saudi Arabia and Beni Suef University, Egypt for the availability of facilities and labs to conduct this research.

References

1. C.H. Caceres, *Metall. Mater. Trans. A*, 38 (2007) 1649.
2. R. Jafar, H. Nouraei, M. Emamifar, M. Papini, and J.K. Spelt, *J Manuf Process*,127 (2015) 17.
3. C. Xu, K. Xia, and T. G. Langdon, *Mater. Sci. Eng. A*,527 (2009) 205.
4. A.A. Abioye, O.P. Abioye, O.O. Ajayi, S.A. Afolalu, M.A. Fajobi, and P.O. Atanda, *Int. J. Mech. Eng. Tech.,* 9 (2018) 694.
5. N. Khayatan, H.M. Ghasemi, and M. Abedini, *Wear,* 380 (2017) 154.
6. D. Zhang, M.M. Wang, N. Jiang, Y. Liu, X.N. Yu, and H.B. Zhang, *Int. J. Electrochem. Sci,* 15 (2020) 4117.
7. B. Barari, E. Omrani, A. Dorri, P.L. Menezes, K.M. Pillai, and P.K. Rohatgi, *Carbohydr Polym.,* 147 (2016) 282.
8. W. Kai, Z. Shengzhe, Z. Yanting, R. Jun, L. Liwei, and L. Yong, *Int. J. Electrochem. Sci*, 13 (2018)

10766.
9. C. Xu, and T.G. Langdon, *J. Mater. Sci.,* 42 (2007) 1542.
10. F. Djavaanroodi and F. Almufadi, *Int. J. Chem. Nucl. Mater. Metall. Eng,* 8 (2014) 3.
11. A. Esmaeili, M.H. Shaeri, M.T. Noghani, and A. Razaghian, *J. Alloys Compd.,* 757 (2018) 324.
12. T.L. Zhilyaev, *Prog. Mater. Sci.,* 53 (2008) 893.
13. C.T. Wang, N. Gao, M.G. Gee, R.J. Wood, and T.G. Langdon, *Wear,* 280 (2012) 28.
14. A.K. Padap, N. Kumar, D. Gupta, and A. Saini, *Tribology in Industry,* 39 (2017) 1.
15. L. Niu and Y.F. Cheng, *Corros. Eng., Sci. Technol.,* 44 (2009) 3893.
16. M. Irfan, A. Irfan, and A. Almufadi, *Materials Testing* 61 (2019) 667.
17. K. M. Emran and A.R. Hanna, *Int. J. Electrochem. Sci,* 12 (2017) 6404.
18. Y. Hedberg, M. Norell, P. Linhardt, H. Bergqvist, I. Odnevall, *Int. J. Electrochem. Sci,* 7 (2012) 11655.
19. Y. Liu, J. Mater. Eng. Perform., 20 (2011) 271.
20. N. Jiang, Y. Liu, X.N. Yu, H.B. Zhang, and M.M.Wang, *Int J Electrochem Sci*, 15 (2020) 5520.
21. Sh. Hassani, K.P. Roberts, S.A. Shirazi, J.R. Shadley, E.F. Rybicki, and C. Joia, *Corr. J. Sci. Eng.*, 68 (2012) 26001.
22. P. Ravindran, K. Manisekar, P. Rathika, and P. Narayanasamy, *Materials & Design,* 45 (2013) 561.
23. L. Robbiola, T.M. Tran, P. Dubot, O. Majerus, and K. Rahmouni, *Corros. Sci.,* 50 (2008) 2205.
24. Z. Wu, Y.F. Cheng, L. Liu, W. Lv, and W. Hu, *Corros. Sci,* 98 (2015) 260.
25. W. Huang, Y. Zhou, Z. Wang, Z. Li, and Z. Zheng, *Mater. Res. Express*, 5 (2018) 56525.
26. S.S. Rajahram, T.J. Harvey, and R.J. Wood, *Wear*, 267 (2009) 244.
27. J. Basumatary and R.J. Wood, *Wear*, 376 (2017) 1286.
28. V.V. Stolyarov and L. Rimma, *J. Alloys Compd*., 378 (2004) 233.
29. Z. Valiev, and G. Langdon, *Prog. Mat. Sci*., 51 (2006) 881.
30. M.I. Pastrama, R. Blanchard, J.G. Clement, P. Pivonka, and C. Hellmich, *J. Mechanical Behavior Biomedical Materials*, 84 (2018) 217.
31. B. Figueiredo, and G. Langdon, *Mater. Sci. Eng*. A, 1 (2009) 105.
32. S.M. Fatemi Varzaneh, and A. Zarei Hanzaki, *Mater. Sci. Eng*. A, 528 (2011) 1334.
33. K. Xia, J.T. Wang, X. Wu, G. Chen, and M. Gurvan, *Mater. Sci. Eng*. A, 410 (2005) 324.
34. Z. Horita, T. Fujinami, and T.G. Langdon, *Mater. Sci. Eng*. A, 300 (2001) 142.
35. C. Xu and T.G. Langdon, *Acta Mater*., 55 (2007) 2360.
36. M. Irfan, F. Almufadi, and F. Djavanroodi, *Metall. Mater. Trans.* A, 49 (2018) 5695.
37. M. Irfan, F. Almufadi, Y. Alshataif, and F. Djavanroodi, *Appl. Sci,* 7 (2017) 1250.
38. Y.K. Li, R.F. Zhou, L. Li, H. Xiao, and Y.H. Jiang, *Mater. Res. Express*, 5 (2018) 66517.
39. J.A.Calderon, J.E. Henao, and M.A. Gomez, *Electrochim. Acta*, 124 (2014) 190.
40. M. Janecek, M. Popov, M.G. Krieger, R.J. Hellmig, and Y. Estrin, *Mater. Sci. Eng.* A,462 (2007) 116.
41. T.G. Langdon, *Mater. Sci. Eng.* A, 462 (2007) 3.
42. K. Bryła, T. Dutkiewicz, L. Litynska-Dobrzynska, L.L. Rokhlin, and P. Kurtyka, *Archives Metallurgy and Materials*, 57 (2012) 711.
43. J.Q. Tao, Y.P. Zhang, F.Y. Fan, and Q. Chen, *Defence Technology*, 9 (2013)146.
44. J. Wang, Y. Iwahashi, Z. Horita, M. Furukawa, M. Nemoto, R. Z. Valiev, and T.G. Langdon, *Acta Mater.,* 44 (1996) 2973.
45. C.L. Silva, I.C. Tristao, S. Sabbaghianrad, S.A. Torbati-Sarraf, R.B. Figueiredo, and T.G. Langdon, *Mater. Res*., 20 (2017) 2.
46. J.C. Lee, H.K. Seok, and J.Y. Suh, *Acta Mater*., 50 (2002) 4005.
47. H. Seikh, M. Baig, and A. Rehman, *Appl. Sci.,* 10 (2020) 7776.
48. C.R. Dean, A.F. Young, I. Meric, C. Lee, L.Wang, S. Sorgenfrei, K. Watanabe, T. Taniguchi, P. Kim, K.L. Shepard, and J. Hone, *Nat. Nanotechnol*., 5 (2010) 722.
49. P.S. Jayabharathy, *Pak. J. Biotechnol*, 15 (2018) 71.

50. M. Irfan, and M. Omar, *Metall. Mater. Trans. A*, 50 (2019) 4232.